Bose polaron in spherically symmetric trap potentials: Ground states with zero and lower angular momenta

Kano Watanabe* and Eiji Nakano†
Department of Physics, Kochi University, Kochi 780-8520, Japan

Hiroyuki Yabu‡
Department of Physics, Ritsumeikan University, Kusatsu 525-8577, Siga, Japan

(Received 10 January 2019; published 28 March 2019)

Single-atomic impurities immersed in a dilute Bose gas in the spherically symmetric harmonic trap potentials are studied at zero temperature. In order to find the ground state of the polarons, we present a conditional variational method with fixed expectation values of the total angular momentum operators $\hat{J}^2$ and $\hat{J}_z$ of the system, using a cranking gauge transformation for bosons to move them in the frame co-rotating with the impurity. In the formulation, the expectation value $\langle \hat{J}^2 \rangle$ is shown to be shared in impurity and bosons, but the value $\langle \hat{J}_z \rangle$ is carried by the impurity due to the rotational symmetry. We also analyze the ground-state properties numerically obtained in this variational method for the system of the attractive impurity-boson interaction, and find that excited boson distributions around the impurity overlap largely with impurity's wave function in their quantum-number spaces and also in the real space because of the attractive interaction employed.

DOI: 10.1103/PhysRevA.99.033624

I. INTRODUCTION

Recently much attention has been devoted to atomic impurities embedded in ultracold atomic media because of experimental accessibility of such systems in controlled ways and of observations of various kinds of quasiparticle properties of the impurities: bosonic [1–7] and fermionic [8–10] ones. For instance, the coupling between impurities and medium can be tuned using the Fano-Feshbach resonances between atomic hyperfine states, and the spatial dimensionality or periodicity of the system can also be designed using the effects of external electromagnetic fields [11,12]. The quasiparticle energy, width, and spectral weight of the impurity can be measured in radio-frequency spectroscopy [5,6,8], and the fine energy splitting of a trapped impurity be measured in the Ramsey spectroscopy with oscillating fields [7]. Also, the dynamical aspects of the polaron formation can be observed experimentally [10].

Theoretical studies of such systems have been actively performed prior to the experiments and revealed that properties of impurity are diverse depending on the impurity-medium interaction and medium properties: When the medium is a Bose-Einstein condensate (BEC), the impurity interacting through the Bogoliubov phonon of the medium is called a Bose polaron [13–34] in analogy with that in electron-phonon systems [35–37], where the atomic impurity is a quasiparticle dressed with a virtual cloud of excited phonons. In the case of a degenerate Fermi-gas medium, the impurity is called Fermi polaron [38–59], which is dressed with particle-hole excitations around the Fermi surface. In these studies the low energy s-wave contact interaction has been frequently used for the impurity-medium interaction. Other kinds of atomic polarons are also studied with unconventional impurity-medium interactions, e.g., p-wave interactions [60,61] and dipolar-dipolar interactions [62,63]. In the case of the impurity-medium coupling tuned around the unitarity limit, the impurity and medium atoms can form few-body bound states in the medium [20,28,55], and consequently the quasiparticle residue almost vanishes. The above mentioned studies entirely assume zero temperature, but recently thermal evolutions of polarons have been investigated, where the medium temperature varies from cold degenerate to hot Boltzmann regimes for Fermi polarons [64–66], and, for Bose polarons, the temperature varies over the BEC critical temperature [67,68].

In many studies of the polaron that have been done so far, the system is assumed to be spatially uniform, while the real experiments of the ultracold gas are usually done on the systems trapped in the harmonic potentials. In the present study we consider a Bose polaron in a spherically symmetric trap in three dimensions, where the angular momentum of the polaron gives the conserved quantum numbers instead of spacial momenta in the uniform system. In particular, we calculate the ground-state energy of a trapped Bose polaron of fixed total angular momentum, and make clear the distributions of the angular-momentum and other quantum numbers of the polaron between the impurity and excited bosons in medium. For this purpose, we develop a variational method with the fixed expectation value of the angular momentum operators.

In Sec. II we set up our system, and derive a Fröhlich type effective Hamiltonian. In Sec. III we introduce a cranking gauge transformation, by which all bosons in medium are cranked to move in the co-rotating frame of impurity.

*b17m6c17m@kochi-u.ac.jp
†e.nakano@kochi-u.ac.jp
‡yabu@se.ritsumei.ac.jp

 ©2019 American Physical Society

In Sec. IV we develop a variational method to obtain the energy functional for the cranked Hamiltonian, and present variational solutions and distribution functions of the excited bosons. In Sec. V numerical results and discussion for them are shown. Section VI is for the summary and outlook.

II. FRÖHLICH TYPE EFFECTIVE HAMILTONIAN

We consider the system of a single atomic impurity interacting with a dilute Bose gas, where the impurity and the gas are trapped in the spherically symmetric harmonic potentials with the same centers. The impurity and bosons are all spinless, so that the total orbital angular momentum of the system is conserved. We also suppose that bosons are noninteracting, while the impurity-boson interaction is tuned finite by the Feshbach resonance method. Thus, when the interaction is turned off, all medium bosons occupy the lowest energy state of the trap potential to form a $T = 0$ BEC. This system is described by the following effective Hamiltonian:

$$\begin{aligned}\mathcal{H}(\mathbf{r}) &= H_{\rm ho}(\mathbf{r}) + \int_{\mathbf{r}'} \phi^\dagger(\mathbf{r}')\left[-\frac{\hbar^2\nabla'^2}{2m_b} + \frac{m_b\omega_b^2}{2}r'^2\right]\phi(\mathbf{r}') \\ &\quad + g\int_{\mathbf{r}'} \phi^\dagger(\mathbf{r}')\delta^{(3)}(\mathbf{r}-\mathbf{r}')\phi(\mathbf{r}') \\ &= H_{\rm ho}(\mathbf{r}) + \sum_s E_s^b b_s^\dagger b_s + g\sum_{s,s'}\phi_s^{b*}(\mathbf{r})\phi_{s'}^b(\mathbf{r})b_s^\dagger b_{s'}, \quad (1)\end{aligned}$$

where the freedoms of the impurity and medium boson are represented in the first and the second quantized form. We have used the abbreviated notation for the spacial integral: $\int_{\mathbf{r}} \equiv \int d\mathbf{r}^3$. The first term $H_{\rm ho}(\mathbf{r})$ is the Hamiltonian of the impurity trapped in the harmonic-oscillator potential:

$$H_{\rm ho}(\mathbf{r}) = -\frac{\hbar^2}{2m_I}\frac{1}{r^2}\partial_r(r^2\partial_r) + \frac{\hbar^2\hat{L}^2}{2m_I r^2} + \frac{m_I\omega_I^2}{2}r^2, \quad (2)$$

where (r, θ, φ) is the spherical coordinate of the impurity, and m_I and ω_I are the impurity mass and the angular frequency of the trap. The squared orbital angular-momentum operator L^2 is represented by

$$\hat{L}^2 = -\left[\frac{1}{\sin\theta}\partial_\theta(\sin\theta\,\partial_\theta) + \frac{1}{\sin^2\theta}\partial_\varphi^2\right].$$

The second term in (1) represents the Hamiltonian of the medium boson; the m_b and ω_b are the mass and the trap angular frequency of the medium boson, and the coupling constant g of the impurity-medium contact interaction is given by the s-wave scattering length a as $g = 2\pi a/m_r$ in low-temperature approximation. The second line of (1) is obtained with the substitution of the field operator expansion $\phi(\mathbf{r}') = \sum_s \phi_s^b(\mathbf{r}')b_s$ where the $\phi_s^b(\mathbf{r})$ are the eigenfunctions of the harmonic oscillator potential for the eigenvalues E_s^b, and the b_s and $b_s^\dagger$ are the corresponding bosonic annihilation and creation operators. The label s representing the medium-boson states is the abbreviated notation for $s = (n, l, m)$: the principal, the azimuthal, and the magnetic quantum numbers, respectively.

The explicit form of the harmonic-oscillator eigenfunctions $\phi_s^\alpha(\mathbf{r})$ for the medium boson ($\alpha = b$) and the impurity ($\alpha = I$) are denoted as

$$\phi_s^\alpha(\mathbf{r}) = R_{nl}^\alpha(r)Y_{lm}(\theta, \varphi), \quad (3)$$

where the angular part Y_{lm} is the spherical harmonic Y function, and the radial part $R_{nl}^\alpha(r)$ are

$$R_{nl}^\alpha(r) = \mathcal{N}_{n,l}(m_\alpha\omega_\alpha)^{3/4}(\sqrt{m_\alpha\omega_\alpha}r)^l\, e^{-\frac{m_\alpha\omega_\alpha}{2}r^2}L_n^{(\frac{1+2l}{2})}(m_\alpha\omega_\alpha r^2), \quad (4)$$

$$\mathcal{N}_{nl} = \sqrt{\frac{2^{n+l+2}n!}{\sqrt{\pi}(2n+2l+1)!!}}. \quad (5)$$

The Laguerre function $L_n^{(k)}(x)$ that we use in this paper is defined by

$$L_n^{(k)}(x) = \frac{e^x x^{-k}}{n!}\frac{d^n}{dx^n}(e^{-x}x^{n+k}).$$

The energy-eigenvalue corresponding to the state (3) is

$$E_{nl}^\alpha = \frac{\omega_\alpha\hbar}{2}(3 + 2l + 4n). \quad (6)$$

It should be noticed that we use the unit system of $\hbar = 1$ throughout this paper.

Bogoliubov approximation and Fröhlich type Hamiltonian: In the case of the small number excitation of medium bosons around the impurity in comparison with the total condensed boson number N_0 [69,70], we can use the Bogoliubov approximation $b_0 \simeq \sqrt{N_0}$, where $s = 0$ corresponds to the lowest energy level ($n = l = 0$). With keeping terms in the interaction part up to the linear order of the excited boson, we obtain

$$\begin{aligned}\mathcal{H}(\mathbf{r}) &\simeq H_{\rm ho}(\mathbf{r}) + E_0^b N_0 + \sum_{s\neq 0} E_s^b b_s^\dagger b_s + gN_0\left|\phi_0^b(\mathbf{r})\right|^2 \\ &\quad + g\sqrt{N_0}\sum_{s\neq 0}[\Phi_s(\mathbf{r})b_s + \Phi_s^*(\mathbf{r})b_s^\dagger], \quad (7)\end{aligned}$$

where

$$\Phi_{s=\{n,l,m\}}(\mathbf{r}) \equiv \sqrt{\frac{1}{4\pi}}R_{00}^b(r)R_{nl}^b(r)Y_{lm}(\theta, \varphi).$$

The Hamiltonian (7) can be transformed into the same form of the Fröhlich Hamiltonian of the electron-phonon system, and the electron polaron was originally studied in [37] for the polar crystals. We will use the Hamiltonian (7) in the present paper.

III. CRANKING OF BOSON STATES

In the present study we aim to find the lowest energy state of the Hamiltonian (7) for given expectation values of the total angular momentum operators. These states correspond to the yrast states appeared in the description of rotational collective excitations of an axially deformed nucleus in nuclear physics, where the rotation axis is not parallel to that of the axially symmetry, and the gauge transformation (cranking) $e^{i\omega_k t\hat{J}_k}$ is introduced conveniently to shift the state from the normal space-fixed frame to the co-rotating frame with the nucleons in which the nucleus wave function is stationary [71–73]. The same method can also be utilized in the present case to describe the excitations of bosons around the impurity; we

rotate the boson cloud around the impurity collectively by the gauge transformation (S transformation) with the solid angle variables (θ, φ) of the impurity:

$$S(\varphi, \theta) = e^{-i\varphi\hat{M}_z} e^{-i\theta\hat{M}_y}, \tag{8}$$

where the boson angular-momentum operator is defined by

$$\hat{M}_i = \sum_{n,l,m,m'} b^\dagger_{nlm} (\hat{\mathcal{L}}_i)^{(l)}_{m,m'} b_{nlm'}, \tag{9}$$

where $(\hat{\mathcal{L}}_i)^{(l)}_{m,m'}$ is the matrix element of a general orbital angular momentum operator $\hat{\mathcal{L}}_i$ by the eigenstates of rank l:

$$\begin{aligned}(\hat{\mathcal{L}}_i)^{(l)}_{m,m'} &\equiv \langle l, m|\hat{\mathcal{L}}_i|l, m'\rangle,\\ l &= 0, 1, 2, \ldots,\\ m, m' &= -l, -1+1, \ldots, l-1, l.\end{aligned}$$

The general form of this transformation has been successfully introduced by Schmidt and Lemeshko to investigate the angular momentum distribution in the system of a linear rotor impurity embedded in bosonic environment in free space [74–76], and the simpler version $S(\varphi, 0)$ has been utilized in the system of Bose polaron in axially symmetric trap potentials for the study of the angular-momentum drag effect [77].

A. Cranked angular momentum operators

The S transformation practically serves as linear transformations for the boson annihilation operators and the boson angular-momentum operators:

$$S^{-1} b_{nlm} S = \sum_{m'=-l,\cdots,l} D^l_{m,m'}(\varphi, \theta, 0) b_{nlm'}, \tag{10}$$

$$S^{-1} \hat{M}_i S = \sum_{j=0,\pm1} {D^1_{i,j}}^*(\varphi, \theta, 0) \hat{M}_j, \tag{11}$$

where we have used the spherical basis: $\hat{M}_0 = \hat{M}_z$ and $\hat{M}_{\pm1} = \mp\frac{1}{\sqrt{2}}(\hat{M}_x \pm i\hat{M}_y)$, for vector indices, and Wigner's D function with Euler angles (α, β, γ) for the spacial rotation [78]:

$$D^l_{m,m'}(\alpha, \beta, \gamma) = \langle l, m| e^{-i\alpha\hat{\mathcal{L}}_z} e^{-i\beta\hat{\mathcal{L}}_y} e^{-i\gamma\hat{\mathcal{L}}_z} |l, m'\rangle. \tag{12}$$

The S transformation acts as a shift operator for the impurity angular-momentum operators:

$$S^{-1}\hat{L}_0 S = \hat{L}_0 + S^{-1}(\hat{L}_0 S) = \hat{L}_0 - S^{-1}\hat{M}_z S, \tag{13}$$

$$\begin{aligned}S^{-1}\hat{L}_{\pm1} S &= \hat{L}_{\pm1} + S^{-1}(\hat{L}_{\pm1} S)\\ &= \hat{L}_{\pm1} + \frac{1}{\sqrt{2}} e^{\pm i\varphi} S^{-1}[i\, e^{-i\varphi\hat{M}_z}\hat{M}_y e^{i\varphi\hat{M}_z} \mp \cot\theta \hat{M}_z] S,\end{aligned} \tag{14}$$

where we have used the spherical-basis representation:

$$\hat{L}_0 = \hat{L}_z = -i\partial_\varphi, \tag{15}$$

$$\hat{L}_{\pm1} = \mp\frac{1}{\sqrt{2}}(\hat{L}_x \pm i\hat{L}_y) = \frac{1}{\sqrt{2}} e^{\pm i\varphi}(-\partial_\theta \mp i\cot\theta\partial_\varphi). \tag{16}$$

In the present system, the total angular momentum operator of the system is given by

$$\hat{J}_i = \hat{L}_i + \hat{M}_i, \tag{17}$$

and the zth component $\hat{J}_z$ and the squared amplitude $\hat{J}^2$ are conserved: $[\hat{J}_z, \mathcal{H}(\mathbf{r})] = [\hat{J}^2, \mathcal{H}(\mathbf{r})] = [\hat{J}_z, \hat{J}^2] = 0$. Using the transformation formulas of the angular momentum operators $\hat{M}_i$ and $\hat{L}_i$, the S-transformed operators of $\hat{J}_z$ and $\hat{J}^2$ becomes

$$S^{-1}\hat{J}_z S = S^{-1}(\hat{L}_z + \hat{M}_z) S = \hat{L}_z, \tag{18}$$

$$\begin{aligned}S^{-1}\hat{J}^2 S &= S^{-1}(\hat{L}^2 + \hat{M}^2 + 2\hat{M}\cdot\hat{L}) S\\ &= \hat{L}^2 + \hat{O}_L + \hat{M}^2\\ &\quad + 2\sum_{i,j=0,\pm1} \hat{M}^\dagger_j D^1_{i,j}(\varphi, \theta, 0)[S^{-1}(\hat{L}_i S) + \hat{L}_i],\end{aligned} \tag{19}$$

where we used the scalar product $\hat{M}\cdot\hat{L} = \sum_{i=0,\pm1} \hat{M}^\dagger_i \hat{L}_i$ in the spherical basis representation, and the shift operator $\hat{O}_L$ of $\hat{L}^2$ is defined by

$$\hat{O}_L := S^{-1}\hat{L}^2 S - \hat{L}^2 = S^{-1}(\hat{L}^2 S) + 2S^{-1}(\hat{L}S)\cdot\hat{L}. \tag{20}$$

We see from the results (18) and (19) that the z component of the total angular momentum is taken over solely by the impurity after the S transformation, while the total angular momentum of the system looks complicated.[1]

B. Cranked Hamiltonian

In a similar calculation, the S transformation of the Hamiltonian (7) is obtained:

$$\begin{aligned}S^{-1}\mathcal{H}(\mathbf{r}) S &= H_{\rm ho}(\mathbf{r}) + \frac{\hat{O}_L}{2m_I r^2} + {\sum_{n,l,m}}' E^b_{nl} b^\dagger_{nlm} b_{nlm}\\ &\quad + E^b_{00} N_0 + g N_0 |\phi^b_0(\mathbf{r})|^2\\ &\quad + g\frac{\sqrt{N_0}}{4\pi} R^b_{00}(r) {\sum_{n,l}}' \sqrt{2l+1} R^b_{nl}(r)(b_{nl0} + b^\dagger_{nl0}),\end{aligned} \tag{21}$$

where the symbols $\sum'_{n,l,m}$ and $\sum'_{n,l}$ represent the summations except $n = l = m = 0$ and $n = l = 0$, respectively. In the derivation we have used the formula $Y^*_{lm}(\theta, \varphi) = \sqrt{\frac{2l+1}{4\pi}} D^l_{m,0}(\varphi, \theta, 0)$ and the orthogonality of the D functions [78]. The second term including the shift operator $\hat{O}_L$ corresponds to the rotation energy of the impurity, which comes from the rotation energy of excited bosons originally before the cranking. The last term is that of the boson-impurity coupling; it should be noticed that it includes the coupling with the excited bosons with $m = 0$ in the S-transformed Hamiltonian [74,75].

[1] In the case of the linear rotor impurity [74,75] the total angular momentum operator is transformed to be that of the impurity, which is by virtue of the intrinsic angular momentum of the rotor itself.

IV. VARIATIONAL METHOD

Let us develop the variational method to obtain the lowest energy states under the condition that the azimuthal and z (magnetic) components of the total angular momentum are given by the expectation values (J, J_z). The Hamiltonian (21) shows that the impurity-boson interaction term includes only the excited bosons with $m = 0$ after the S transformation, so that, as a variational state of excited bosons around the impurity, we employ the coherent state for the excited bosons with the quantum numbers $s = (n, l, 0)$ [79,80]:

$$|b\rangle = \exp \sum_{n,l}{}' (f_{nl} b^\dagger_{nl0} - f^*_{nl} b_{nl0})|0\rangle, \tag{22}$$

where the variational parameters f_{nl} and f^*_{nl} are eigenvalues of annihilation and creation operators: $b_{nl0}|b\rangle = f_{nl}|b\rangle$, $\langle b|b^\dagger_{nl0} = \langle b|f^*_{nl}$. The state $|b\rangle$ is a normalized one: $\langle b|b\rangle = 1$. It would be a good approximation for the heavy impurity trapped in the deep potential; in the case of heavy mass or high trap-frequency limits of the impurity, the above coherent state becomes the exact solution because the impurity becomes localized at the center of trap.[2]

Now we use the abbreviated notation for the expectation value of operator by the coherent state $|b\rangle$ as $\langle \cdots \rangle_b \equiv \langle b| \cdots |b\rangle$. Then that of the transformed Hamiltonian (21) and the S-transformed total angular momentum operators become

$$\begin{aligned}
&\langle S^{-1}\mathcal{H}(\mathbf{r})S\rangle_b \\
&= H^f_{\rm ho}(\mathbf{r}) + \sum_{n,l}{}' \left[\frac{l(l+1)}{2m_I r^2} + E^b_{nl}\right]|f_{nl}|^2 \\
&\quad + E^b_{00}N_0 + gN_0\left|\phi^b_0(\mathbf{r})\right|^2 \\
&\quad + g\frac{\sqrt{N_0}}{4\pi}R^b_{00}(r)\sum_{n,l}{}' \sqrt{2l+1}R^b_{n,l}(r)(f_{nl} + f^*_{nl}),
\end{aligned} \tag{23}$$

$$\langle S^{-1}\hat{J}^2 S\rangle_b = \hat{L}^2, \tag{24}$$

$$\langle S^{-1}\hat{J}_z S\rangle_b = \hat{L}_z, \tag{25}$$

where we have used the expectation value $\langle \hat{O}_L\rangle_b = \sum'_{n,l} l(l+1)|f_{nl}|^2$.[3]

The expectation value (23), where the bosonic degrees of freedom have been eliminated, provide the effective Hamiltonian of the impurity, and Eqs. (24) and (25) are the corresponding effective total angular-momentum operators represented with the impurity coordinate. It is very interesting that the latter are the same with the impurity angular momentum; it gives an essential advantage in the present variational method with the condition of the fixed total angular momentum.

A. Variational states of impurity

Since the total angular momentum operators (24) and (25) are given by those of the impurity, the variational state of the impurity can be assumed as the eigenfunctions (3) of the impurity with fixed azimuthal and magnetic quantum numbers (J, J_z):

$$\Psi_{JJ_z}(\mathbf{r}) = \sum_n F_{nJJ_z}\,\phi^I_{nJJ_z}(\mathbf{r}), \tag{26}$$

where $J_z = -J, -J+1, \ldots, J-1, J$ and the coefficients F_{nJJ_z} serve as Ritz-type variational parameters. Note that we do not consider mixing of different angular momenta, because of rotational symmetry. Since the states with large principal quantum numbers contribute less in the ground state in the weak coupling regime, we truncate the variational state up to $n = 1$ in the present calculation:

$$\Psi_{JJ_z}(\mathbf{r}) = \sum_{n=0,1} F_{nJ}\,\phi^I_{nJJ_z}(\mathbf{r}). \tag{27}$$

Note that the subscript J_z has been omitted in the variational parameters since the rotational symmetry of the system gives the degeneracy for the direction in real space and the variational parameters do not depend on J_z. In solving the variational equations, we impose the normalization condition for the parameters: $|F_{0J}|^2 + |F_{1J}|^2 = 1$.

B. Variational energy functional and solutions

Now taking the expectation value of the Hamiltonian (23) with respect to the impurity's variational state (27), we obtain the variational energy functional for the state with the total angular momentum (J, J_z):

$$\begin{aligned}
&E[F_{nJ}; f_{nl}] \\
&= \langle \mathcal{H}(\mathbf{r})\rangle_{JJ_z} \\
&= E^I_{0J}|F_{0J}|^2 + E^I_{1J}|F_{1J}|^2 + E^b_{00}N_0(|F_{0J}|^2 + |F_{1J}|^2) \\
&\quad + \sum_{n,l}{}' \left[E^b_{nl}(|F_{0J}|^2 + |F_{1J}|^2) + \frac{l(l+1)}{2m_I}G[F_{0J}; F_{1J}]\right]|f_{nl}|^2 \\
&\quad + g\frac{N_0}{4\pi}H[F_{0J}; F_{1J}]_{00} \\
&\quad + g\frac{\sqrt{N_0}}{4\pi}\sum_{n,l}{}' \sqrt{2l+1}[H[F_{0J}; F_{1J}]_{nl} f_{nl} \\
&\quad + H[F_{0J}; F_{1J}]^*_{nl} f^*_{nl}],
\end{aligned} \tag{28}$$

where we have defined the functionals:

$$G[F_{0J}; F_{1J}] = \int_{\mathbf{r}} \frac{1}{r^2}\left|\sum_{n=0,1} F_{nJ}\phi^I_{nJJ_z}(\mathbf{r})\right|^2, \tag{29}$$

$$H[F_{0J}; F_{1J}]_{nl} = \int_{\mathbf{r}} R^b_{00}(r)R^b_{nl}(r)\left|\sum_{n=0,1} F_{nJ}\phi^I_{nJJ_z}(\mathbf{r})\right|^2. \tag{30}$$

The variational equation $\delta E/\delta f^*_{nl} = 0$ gives the formal solution:

$$\begin{aligned}
&\bar{f}_{nl}[F_{0J}; F_{1J}] \\
&= -g\frac{\sqrt{N_0}}{4\pi}\frac{\sqrt{2l+1}H[F_{0J}; F_{1J}]^*_{nl}}{E^b_{nl}(|F_{0J}|^2 + |F_{1J}|^2) + \frac{l(l+1)}{2m_I}G[F_{0J}; F_{1J}]},
\end{aligned} \tag{31}$$

[2] A marginal case where $m_I \to \infty$ as $m_I\omega_I^2$ is kept finite is also soluble.

[3] For derivations of the expectation values, see Appendix A.

and, plugging it back to the variational energy (28), we obtain

$$E[F_{nJ};\bar{f}_{nl}] = E^I_{0J}|F_{0J}|^2 + E^I_{1J}|F_{1J}|^2 + E^b_{00}N_0(|F_{0J}|^2+|F_{1J}|^2) + g\frac{N_0}{4\pi}H[F_{0J};F_{1J}]_{00} - g^2\frac{N_0}{(4\pi)^2}{\sum_{n,l}}'(2l+1) \times \frac{|H[F_{0J};F_{1J}]_{nl}|^2}{E^b_{nl}(|F_{0J}|^2+|F_{1J}|^2)+\frac{l(l+1)}{2m_I}G[F_{0J};F_{1J}]}.$$

Since the coefficients appearing in the variational energy are all real, the solutions of F_{0J} and F_{1J} are also found to be real. Using the normalization condition $F_{0J}=\sqrt{1-F^2_{1,J}}$ and the analytical expression[4] of $G[F_{0J};F_{1J}]$, we finally obtain

$$E[F_{1J}] = E^I_{0J} + E^b_{00}N_0 + \left(E^I_{1J}-E^I_{0J}\right)F^2_{1J} + E_{\rm bg}[F_{1J}] + E_{\rm int}[F_{1J}], \tag{32}$$

where the background interaction energy is

$$E_{\rm bg}[F_{1J}] \equiv g\frac{N_0}{4\pi}\left[H^0_{00J} + 2F_{1J}\sqrt{1-F^2_{1J}}H^c_{00J} + F^2_{1J}\left(H^1_{00J}-H^0_{00J}\right)\right], \tag{33}$$

which comes from the interaction between impurity and background condensed bosons corresponding to the term $gN_0|\phi^b_0(\mathbf{x})|^2$ in (23). The interaction energy term $E_{\rm int}[F_{1J}]$ is represented as

$$E_{\rm int}[F_{1J}] \equiv -\frac{g^2N_0}{(4\pi)^2}{\sum_{n,l}}'(2l+1) \times \frac{\left[H^0_{nlJ}+2F_{1J}\sqrt{1-F^2_{1J}}H^c_{nlJ}+F^2_{1J}\left(H^1_{nlJ}-H^0_{nlJ}\right)\right]^2}{E^b_{nl}+\frac{l(l+1)}{2J+1}\omega_I\left[1+2F_{1J}\sqrt{1-F^2_{1J}}/\sqrt{J+\frac{3}{2}}\right]}, \tag{34}$$

which is traced back to the parts including f_{nl} in the second and the last terms in (23), and corresponds to the interaction between the impurity and the excited bosons. The explicit forms of the coefficients H^0_{nlJ}, H^c_{nlJ}, H^1_{nlJ} in $E_{\rm bg}$ and $E_{\rm int}$ are shown also in Appendix B.

In experiments, the energy shift, i.e., the energy with bare impurity and background BEC contributions being subtracted, is measurable using the radio-frequency spectroscopy [5,6]; in the present theory, it is given by the formula

$$\Delta E[F_{1J}] \equiv \left(E^I_{1J}-E^I_{0J}\right)F^2_{1J} + E_{\rm bg}[F_{1J}] + E_{\rm int}[F_{1J}]. \tag{35}$$

C. Comparison with the second-order perturbation theory

In general, the solutions of variational method in the present method includes nonperturbative effects, but it is heuristic and interesting to see its perturbative nature before going into numerical results. Expanding the variational solution (32) with the coupling constant g, we obtain $F_{1J} = -g\frac{N_0}{4\pi}\frac{H^c_{00J}}{E^I_{1J}-E^I_{0J}}$, to the leading order of g; then the ground state energy becomes

$$E = E^I_{0J} + E^b_{00}N_0 + g\frac{N_0}{4\pi}H^0_{00J} - g^2\frac{N_0^2}{(4\pi)^2}\frac{\left(H^c_{00J}\right)^2}{E^I_{1J}-E^I_{0J}} - g^2\frac{N_0}{(4\pi)^2}{\sum_{n,l}}'\frac{(2l+1)\left(H^0_{nlJ}\right)^2}{E^b_{nl}+\frac{l(l+1)}{2J+1}\omega_I} \tag{36}$$

to the order of g^2. The result should be compared with that of the second-order perturbation theory; for the ground state energy of $J=0$:[5]

$$\langle\mathcal{H}\rangle \simeq E^I_{00} + E^b_{00}N_0 + g\frac{N_0}{4\pi}H^0_{000} - g^2\frac{N_0^2}{(4\pi)^2}\frac{\left(H^c_{000}\right)^2}{E^I_{10}-E^I_{00}} - g^2\frac{N_0}{(4\pi)^2}\sum_{n\neq0}\left(\frac{\left(H^c_{n00}\right)^2}{E^I_{10}-E^I_{00}+E^b_{n0}}+\frac{\left(H^0_{n00}\right)^2}{E^b_{n0}}\right). \tag{37}$$

Comparing (36) with (37), we find that differences appear in the g^2N_0 term, which is attributed to the Fröhlich-type boson-impurity interaction. In the denominator of (36), the energy of impurity's intermediate states in (37) is replaced by an averaged rotation energy $\frac{l(l+1)}{2J+1}\omega_I$. It can be explained from the cranking transformation and the angular momentum conservation: after cranking transformation, all bosons stop to be in rotating states, and the impurity rotates instead in order to satisfy the angular momentum conservation; consequently its effect appears as the rotation energy. In the perturbation theory for the ground state, the impurity and bosons intermediate virtual states are taken in the order from those of low-energy regardless of the angular momentum conservation.

D. Distribution functions of excited bosons and quasiparticle residue

Since the quasiparticle properties of the Bose polaron are characterized by the virtual boson excitations around the impurity, the number of excited bosons around the polaron is an important quantity. The excited-boson number $N^{JJ_z}_{nlm}$ of bosons with quantum numbers (n,l,m) for the polaron with the total angular momentum (J,J_z) is given by

$$N^{JJ_z}_{nlm} = \langle b^\dagger_{nlm}b_{nlm}\rangle_{JJ_z} = \int d\theta\sin\theta d\varphi\,|Y_{JJ_z}(\theta,\varphi)|^2\left|D^l_{m,0}(\varphi,\theta,0)\right|^2 \times\langle b|b^\dagger_{nl0}b_{nl0}|b\rangle = |f_{nl}|^2\sum_{L=|J-l|}^{J+l}\langle l0;L0|J0\rangle^2\,\langle JJ_z;lm|LJ_z+m\rangle^2. \tag{38}$$

It should be noted that the dependence on J_z and m in $N^{JJ_z}_{nlm}$ comes through the Clebsch-Gordan coefficients[6] $\langle l0;L0|J0\rangle$ and $\langle JJ_z;lm|LJ_z+m\rangle$ which are originated in the averaged overlap of the coupled angular-momentum states from J and

[4] See Appendix B.

[5] For derivation, see Appendix C.

[6] For the definition of the Clebsch-Gordan coefficients, see [78,81].

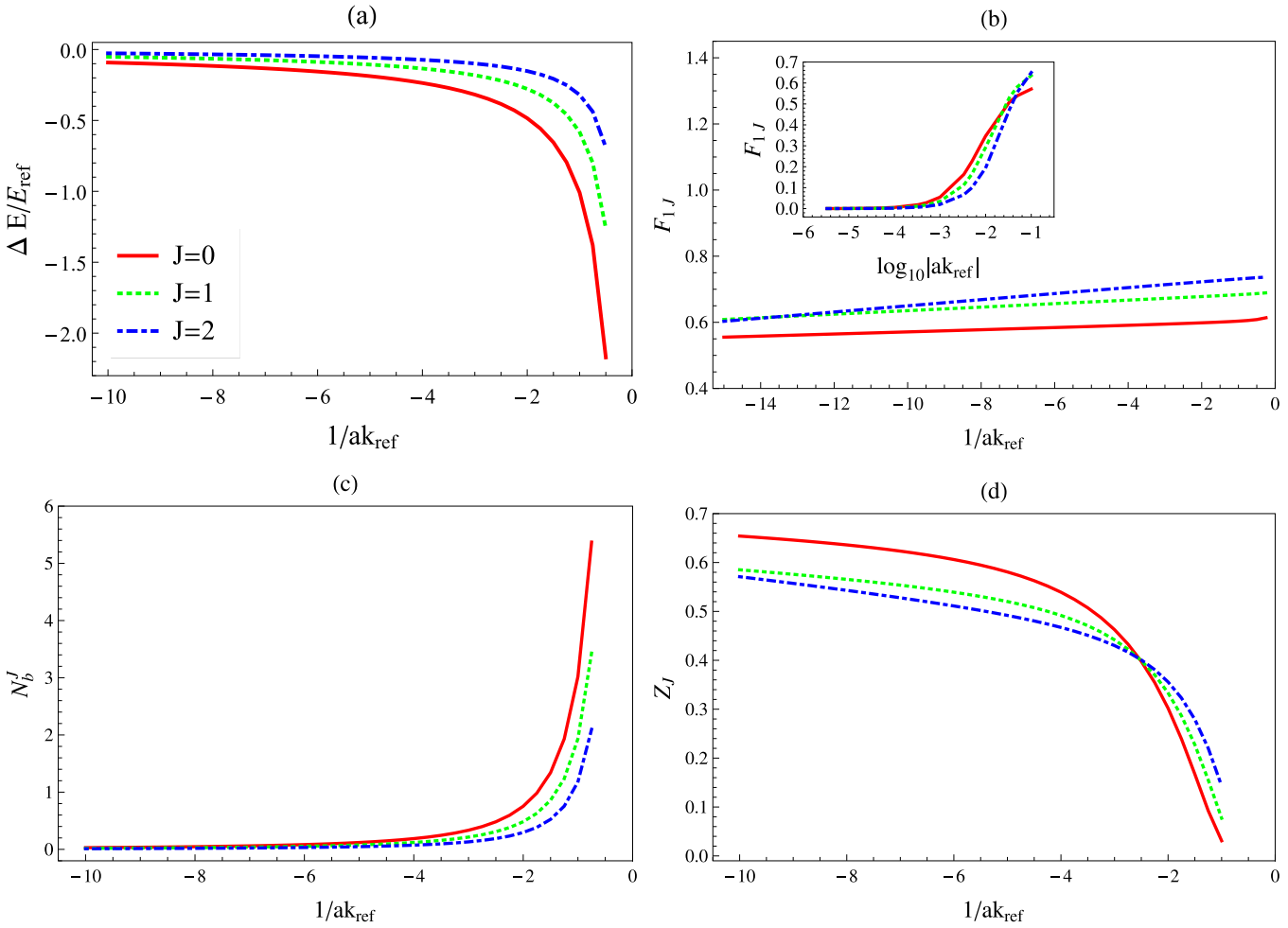

FIG. 1. The energy shift (a), the variational parameter F_{1J} (b), the total excited-boson number (c), and the quasiparticle residue (d) for $J = 0, 1, 2$, as functions of the inverse of scattering length with the parameters in (43). The inset in the (b) is for smaller scattering-length region. The definitions of these quantities are given in (35), (27), (39), and (42), respectively.

l. The dependence through the Clebsch-Gordan coefficients is not dynamical but kinematical; it can be understood from independence of the polaron energy functional on J_z or m.

From (38) we obtain the total excited-boson number by summing up quantum numbers:

$$N_b^J = \sum_{n,l}{}' \sum_{m=-l,\ldots,l} N_{nlm}^{JJ_z} = \sum_{n,l}{}' |f_{nl}|^2. \tag{39}$$

It is clear that the total number does not depend on J_z but it has the implicit J dependence through the variational parameter F_{1J}.

The real-space density distribution of the excited bosons is given by the expectation value:

$$\langle \phi^{b\dagger}(\mathbf{x})\phi^b(\mathbf{x})\rangle_{JJ_z} = \sum_{n,l}{}' \sum_{m=-l,\cdots,l} N_{nlm}^{JJ_z} \left|\phi_{nlm}^b(\mathbf{x})\right|^2. \tag{40}$$

For the angular momentum, the boson contribution is found to vanish,

$$\langle \hat{M}_i\rangle_{JJ_z} = 0, \tag{41}$$

which implies that the impurity alone bears the contribution for J_z; it shows that no drag effects exist for the angular momentum unlike the axial symmetric case [77]. There are two reasons for this property. First, thanks to the complete rotational symmetry the energy functional becomes spherically symmetric and does not depend on J_z. Second, no angular-momentum exchange can happen between impurity and bosons through the impurity-boson interaction because a density-density type interaction is employed in this work. In order for $\langle \hat{M}_i\rangle$ to be finite, an asymmetry with respect to m is required in the distribution function of excited bosons, but there is no sources of the asymmetry in the present case because of the rotational symmetry. In the case of axial symmetric trap potentials, this specific axis provides an asymmetry for the energy functional and the distribution function [77]. We will come back to this point when we present the numerical results in the next section.

The quasiparticle residue is defined as

$$Z_J = \left|\int_{\mathbf{r}} \phi_{0JJ_z}^{I*}(\mathbf{r})\langle 0|S|b\rangle \Psi_{JJ_z}(\mathbf{r})\right|^2 = |F_{0J}|^2 e^{-\sum_{n,l}{}'|f_{nl}|^2}. \tag{42}$$

It also quantifies the modification of the impurity due to the interaction effects, which is given by the overlap between the bare and interacting impurity states with the angular momentum (J, J_z). Equation (42) shows that the residue is factorized into the ground state component of the impurity wave function $|F_{0J}|^2$ and a weight factor $e^{-\sum'_{n,l}|f_{nl}|^2}$ of the excited bosons, while in the spatially uniform case it depends only on the latter.

V. NUMERICAL RESULTS AND DISCUSSION

In numerical calculation we take ^{40}K as the impurity immersed in medium bosons of ^{87}Rb; the trap frequencies of the impurity and the medium bosons and the condensed-boson number that we take are

$$\omega_I = 200\ \text{Hz}, \quad \omega_b = 100\ \text{Hz}, \quad N_0 = 10^4, \tag{43}$$

throughout numerical calculations. We treat the boson-impurity scattering length as a variable parameter, but neglect the boson-boson scattering length in the present calculation. In actual experiments of Bose polarons [5,6], the trap potentials for impurity and medium bosons are both axially symmetric, and the boson-boson scattering length is usually set to be a small positive number to stabilize the boson sector. In the present theoretical study of the idealized system, the zero-point energy in the trap supports and stabilizes the system, and the present system of the negligible boson-boson scattering length can be potentially realized in real experiments.

The average density of condensed bosons in the trap system is defined as

$$\bar{n} = N_0 \int_{\mathbf{r}} \left|\phi_0^b(\mathbf{r})\right|^4 = N_0 \left(\frac{m_b \omega_b}{2\pi}\right)^{3/2}. \tag{44}$$

We also introduce the scale factors for momentum and energy:

$$k_{\text{ref}} = (6\pi^2 \bar{n})^{1/3}, \quad E_{\text{ref}} = \frac{k_{\text{ref}}^2}{2m_b}, \tag{45}$$

as in the case of the uniform systems [6,17,19].

A. The ground state energies for the states of small angular momentum

In Fig. 1 we show the scattering-length dependence of the ground state properties of polaron: the energy shifts (35), the calculated values of impurity's variational parameter F_{1J} in (27), the total number of excited bosons (39), and quasiparticle residue (42), for the small numbers of the total angular momenta ($J = 0, 1, 2$).[7]

The energy shift obtained here should be comparable with the experimental result [6] only for the case of small scattering lengths, roughly of $1/ak_{\text{ref}} < -2$; it is because the Bogoliubov approximation (7) employed here works only if the number of excited bosons is less than or equal to the number of impurities (it is the unity in the present calculation), and also the two-level approximation in the impurity wave function (27) is valid for the smaller values of variational solutions

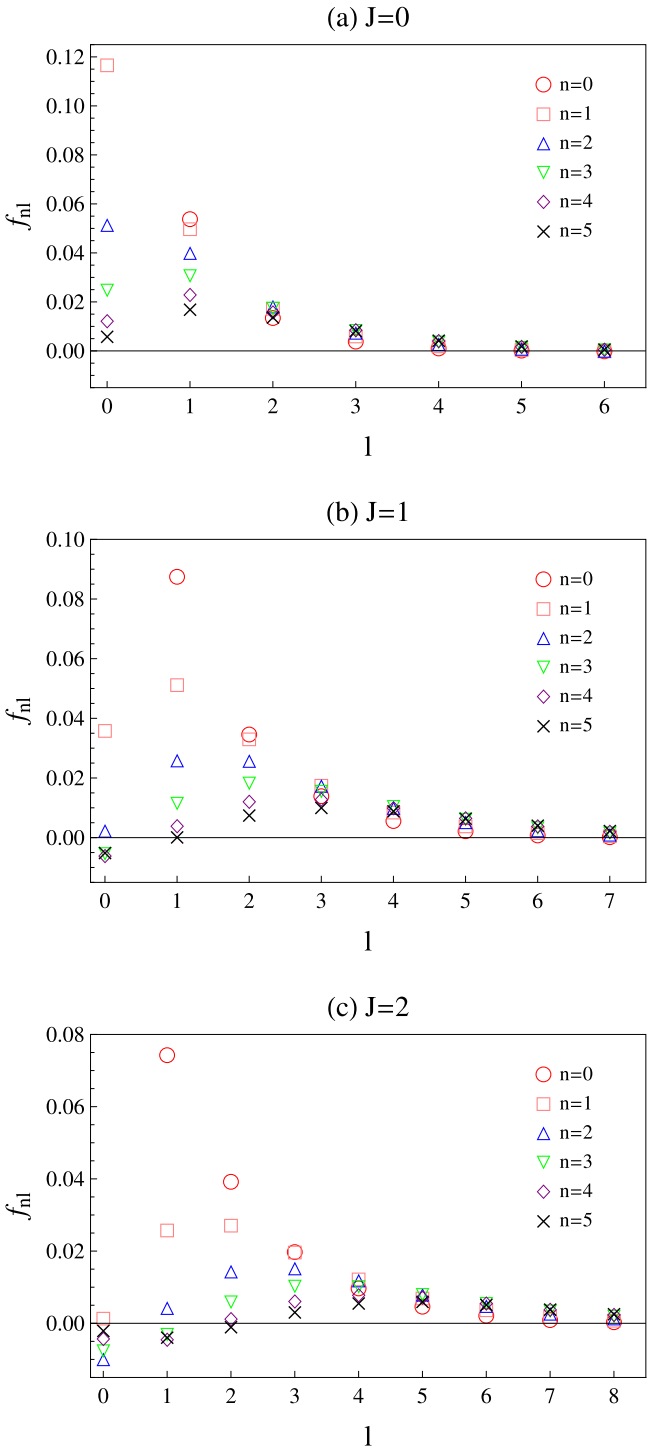

FIG. 2. The variational parameter of excited bosons (31) for $J = 0, 1, 2$ and their angular-momentum l dependencies. A set of parameters is given in (43), and $1/ak_{\text{ref}} = -9.95$.

[7] In these calculations we have taken the approximation to cut the summation in the interaction energy (34) up to $(n, l) = (30, 10)$. We have checked the approximation numerically by raising the maximum values of n and l by 100%; then the numerical results change within a few percent, and the sum of l shows a rapid convergence. Also, since $H_{nlJ}^{0,c,1} \to 0$ as $n \to \infty$ or $l \to \infty$, the series of n, l summation in (34) drop faster than the order of $1/n$ $(1/l)$ for large number of n (l), which implies the series is a convergent one.

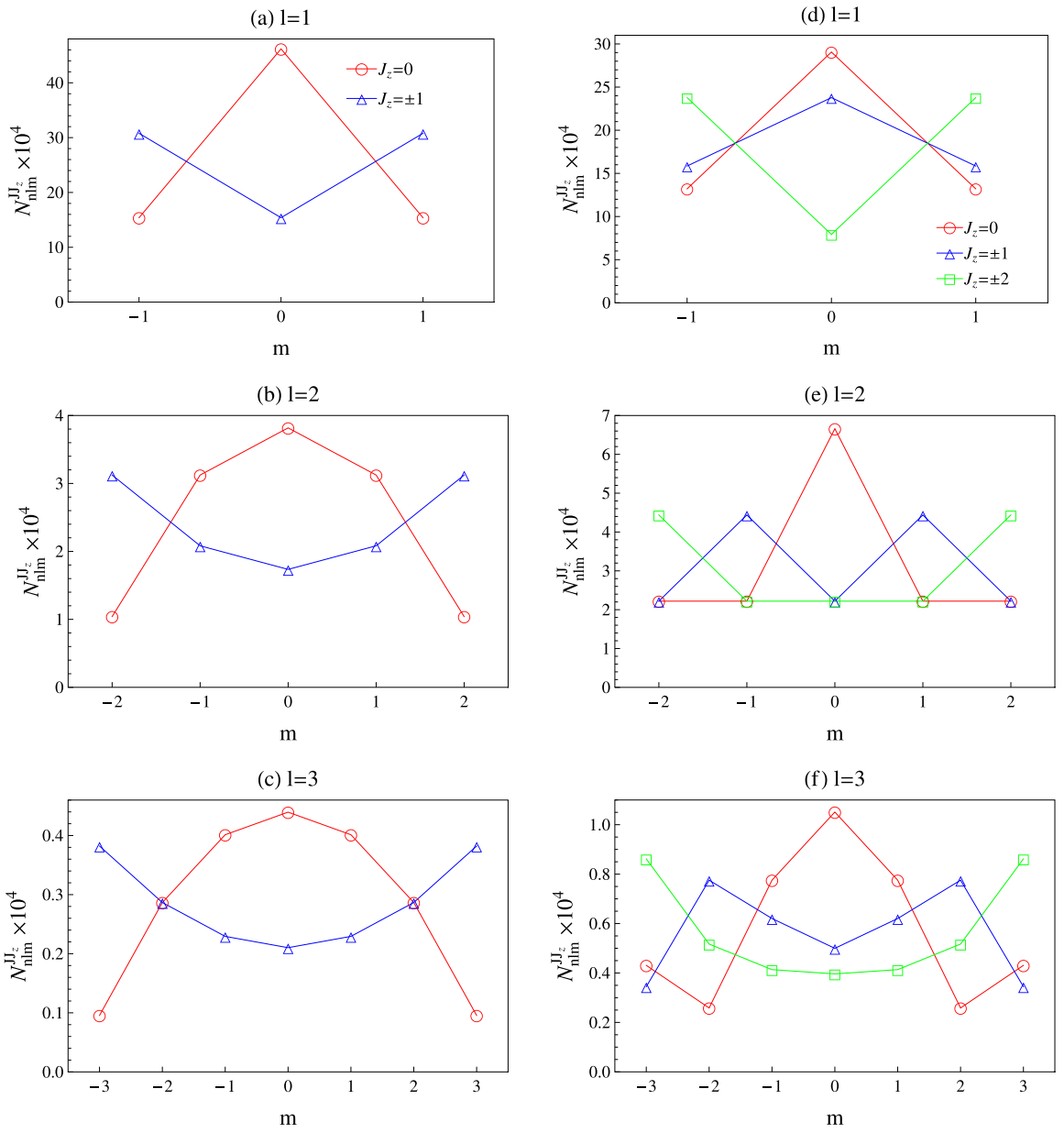

FIG. 3. The angular-momentum (l, m) dependencies of the excited-boson numbers in (38) for $n = 0$ and $l = 1, 2, 3$. (a), (b), and (c) Left and right columns are for $J = 1$ ($J_z = 0, \pm 1$) and $J = 2$ ($J_z = 0, \pm 1, \pm 2$), respectively. The parameter set is the same as in Fig. 2.

($F_{1J} \ll F_{0J}$), and loses the validity when $F_{1J} \gtrsim 1/\sqrt{2} \sim 0.7$.[8] Also, the behavior of the residue implies that quasiparticle picture of the polaron works for about $1/ak_{\rm ref} < -2$ as well. In the case of the strong coupling regime and around the unitary limit, i.e., $|1/ak_{\rm ref}| < 1$, we need to include effects of the two-to-two scattering processes between impurity and excited boson which were discarded in the Bogoliubov approximation; they are responsible for the effective in-medium shift in the unitary limit [28] and the in-medium few-body bound states [20,28].

B. Distributions of excited bosons

In Fig. 2 we show the solutions of variational parameter f_{nl} for $J = 0, 1, 2$, where we have set the impurity-boson scattering length by $a = -5.77$ nm corresponding at $1/ak_{\rm ref} = -9.95$. The parameter f_{nl} can be interpreted as the probability amplitude of excited bosons with the quantum numbers (n, l). These figures implies that, for each principal quantum number n, the peak positions of f_{nl} for the quantum number l move to the right as the total angular momentum J is increased. This is due to the attractive density-density-type interaction between impurity and bosons, which cause the large overlap between

[8]Note that the variational solution of F_{1J} is determined mainly from the first two terms in (35), and takes smaller values in the cases of the heavier impurity masses or of the larger trap frequencies than the present ones.

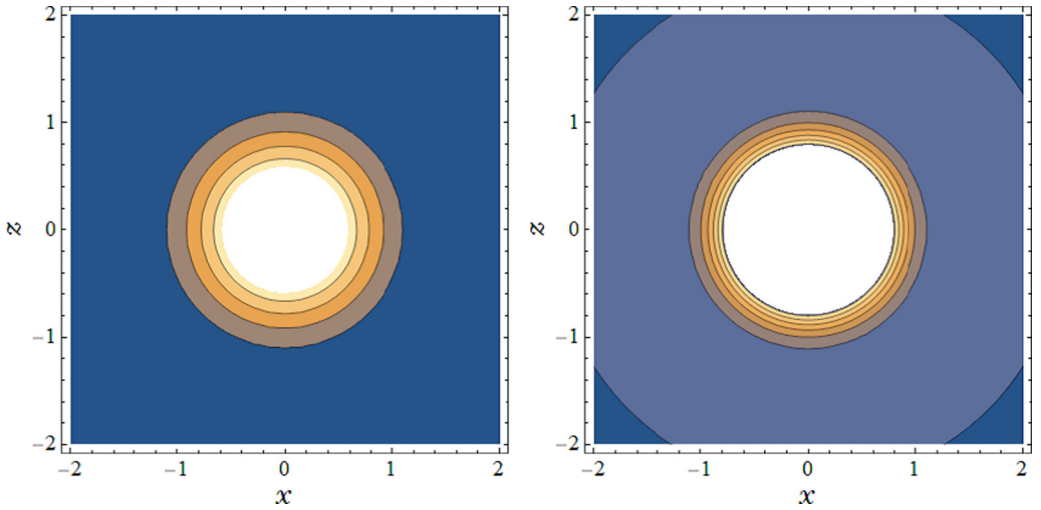

FIG. 4. The $J = J_z = 0$ contour plots of the impurity's probability density $|\Psi_{JJ_Z}(\mathbf{r})|^2$ (left panel) and the real-space excited-boson distributions (right panel) defined in (40), in the cross-section plane of $y = 0$, where the ordinate is the z axis (the direction of the magnetic quantum number), and the abscissa is the x axis. Note that these plots have the rotational symmetry around the z axis. The units of axes are $(\omega_I m_I)^{-1/2}$ (left) and $(\omega_b m_b)^{-1/2}$ (right), and the heights of the contour lines (not shown explicitly) are normalized by $(\omega_I m_I)^{3/2}$ (left) and $(\omega_b m_b)^{3/2}$ (right). The parameter set is the same as in Fig. 2.

their wave functions to lower the interaction energy. It can be shown more directly in the real space distributions (Figs. 4–6).

In Fig. 3 we also show the quantum-number distributions of the excited bosons $N_{nlm}^{JJ_z}$ given by (38) for the states of $J = 1, 2$ as functions of the quantum number m for $l = 1, 2, 3$ and $n = 0$, with the same parameter set as in Fig. 2. As expected from the angular-momentum conservation and no drag effect, i.e., $\langle \hat{M}_z \rangle_{JJ_z} = 0$, in the present calculation, all plots in the figures show that the distributions for the quantum number m are symmetric about $m = 0$. In order to understand the result, let us suppose an impurity prepared in the state with a specific value of $J_z(= L_z)$, which gives a specific direction in the space. If the interaction could be turned off between the impurity and surrounding bosons, the energy of the system should be still degenerate to the value of J_z. However, the presence of the real interaction causes the same number of virtual boson excitations with the quantum number $-|m|$ and $|m|$ in order to gain the interaction energy by a maximal overlap with the impurity (as shown in Figs. 4–6), which leads to the vanishing $\langle \hat{M}_z \rangle_{JJ_z}$.

For a different value of the principal quantum number $n \neq 0$, we have confirmed that the excited-boson number distributions have the completely same shape as that of $n = 0$ since distribution shapes are determined by the Clebsch-Gordan coefficients for a given set of (J, J_z, l, m), which are independent of n, but their intensities decrease with increasing n. The special case is for $J = J_z = 0$, where the factor N_{nlm}^{00} determined from the Clebsch-Gordan coefficients has no m dependence; their numerical values for $l = 1, 2, 3$ are $N_{01m}^{00} = 9.76 \times 10^{-4}$, $N_{02m}^{00} = 0.38 \times 10^{-4}$, and $N_{03m}^{00} = 0.024 \times 10^{-4}$, respectively.

Finally we show in Figs. 4–6 the real space distributions (40) of excited bosons together with impurity's probability density obtained from (27) for the same parameter set as that in Fig. 2. To generate the distributions of excited bosons shown in Figs. 4–6, we have evaluated (40) in the approximation of taking quantum numbers up to $(n, l) = (5, 5)$ in the summation, since f_{nl} of higher quantum numbers does not contribute so much as the variational parameters (Fig. 2). Comparing left and right figures for $J = 0, 1, 2$, we can observe that the attractive impurity-boson interaction has the effect that causes overlaps in their distributions, as discussed just above on the quantum-number distributions. The impurity's probability is proportional to $|Y_{JJ_z}(\theta, \varphi)|^2$, thus the figures clearly exhibit the s, p, and d orbital shapes for $J = 0, 1, 2$, respectively. On the other hand, boson's distributions are blurred because they always include $l = 0$ isotropic contributions as shown in (40) with variationally determined weight factor $|f_{nl}|^2$.

VI. SUMMARY AND OUTLOOK

In this paper we have investigated the ground-state properties of the impurity interacting with medium bosons in spherically symmetric trap potentials, when the total angular momentum (J, J_z) are given. To this end we have developed a conditional variational method, and obtained the ground-state energies, quasiparticle residue of polaron, and the quantum-number and real spaces distributions of excited bosons for the cases of total angular momenta $J = 0, 1, 2$. From theoretical consideration we have found that the expectation value $\langle \hat{J}^2 \rangle_{JJ_z} = J(J + 1)$ is shared by the impurity and the excited bosons as

$$\langle \hat{L}^2 \rangle_{JJ_z} = J(J+1) + \sum_{n,l}{}' l(l+1)|f_{nl}|^2,$$

$$\langle \hat{M}^2 \rangle_{JJ_z} = \sum_{n,l}{}' l(l+1)|f_{nl}|^2,$$

$$\langle 2\hat{L} \cdot \hat{M} \rangle_{JJ_z} = -2 \sum_{n,l}{}' l(l+1)|f_{nl}|^2, \tag{46}$$

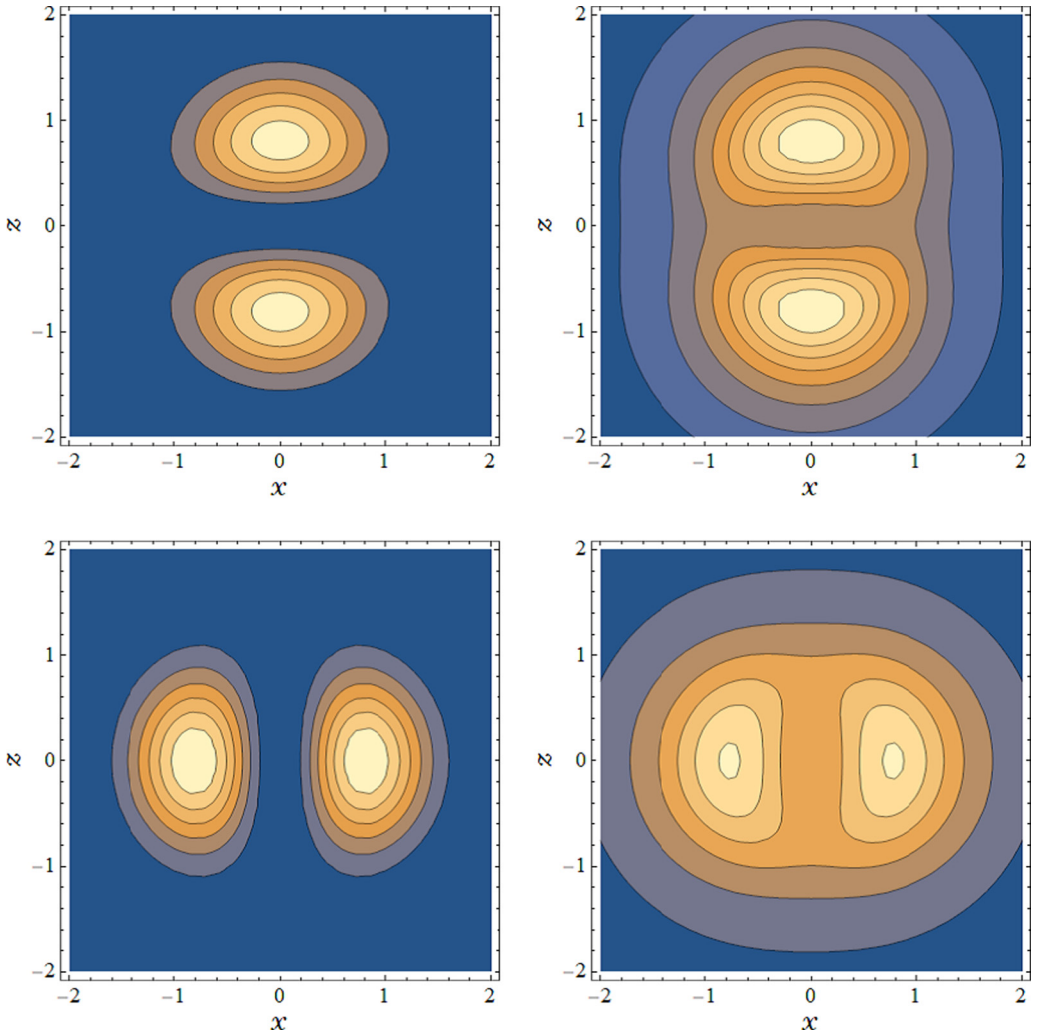

FIG. 5. The $J = 1$ contour plots of the impurity's probability density (left panel) and the real-space excited-boson distributions (right panel): the top and bottom panels are for $|J_z| = 0, 1$. For other explanations, see the caption in Fig. 4.

while that of the zth component $\langle \hat{J}_z \rangle_{JJ_z} = J_z$ comes from the impurity only:

$$\langle \hat{L}_z \rangle_{JJ_z} = J_z, \quad \langle \hat{M}_z \rangle_{JJ_z} = 0, \tag{47}$$

which implies no drag effect for the polaron in the spherically symmetric trap potentials. We have also made numerical calculations based on the variational method, and, as shown in Figs. 2–6, found that the excited bosons are distributed so as to make a large overlap with impurity's probability density in real and quantum-number spaces because of the attractive impurity-boson interaction.

In the present study the excited bosons do not move collectively by themselves [82,83] since no boson-boson interaction is assumed, so they are in purely quantum regime. In most of recent experimental researches, the Bose polarons are realized in the system of the repulsive boson-boson interactions where the medium bosons form a superfluid BEC. In order to analyze such cases, we need Bogoliubov–de Gennes-type approaches [84–89] beyond the Bogoliubov approximation. Such extensions of the present approach for the trapped polaron including the boson-boson interactions should give more detailed polaron's structures such as a local depletion of BEC around impurity as well as the excitation spectra of the bosonic sector.

Finally, we comment a bit on the possibility of experimental observation of the finite angular momentum states of the trapped Bose polaron discussed in this paper. To our knowledge, all experiments have been done with axial-symmetric traps for both impurity and medium atoms, and no angular momentum is given to the atoms in total. To give some finite angular momentum to the system in axial symmetric trap potentials, we expect that the experimental methods of creating a vortex state of the BEC can be utilized [90,91]: rotating a very dilute impurity-atom gas before switching on the interaction with medium bosons, and then the whole system, as Bose polaron, finally acquires some finite angular momentum. Furthermore, if the axial symmetric trap is deformed adiabatically to the spherical one, there remains the state with a finite angular momentum, the quantization axis of which should be the same with that of the original axial symmetry.

For the observation of the angular-momentum distribution of the impurity, the photon absorption spectra for excitations for the states with different angular momenta can be utilized,

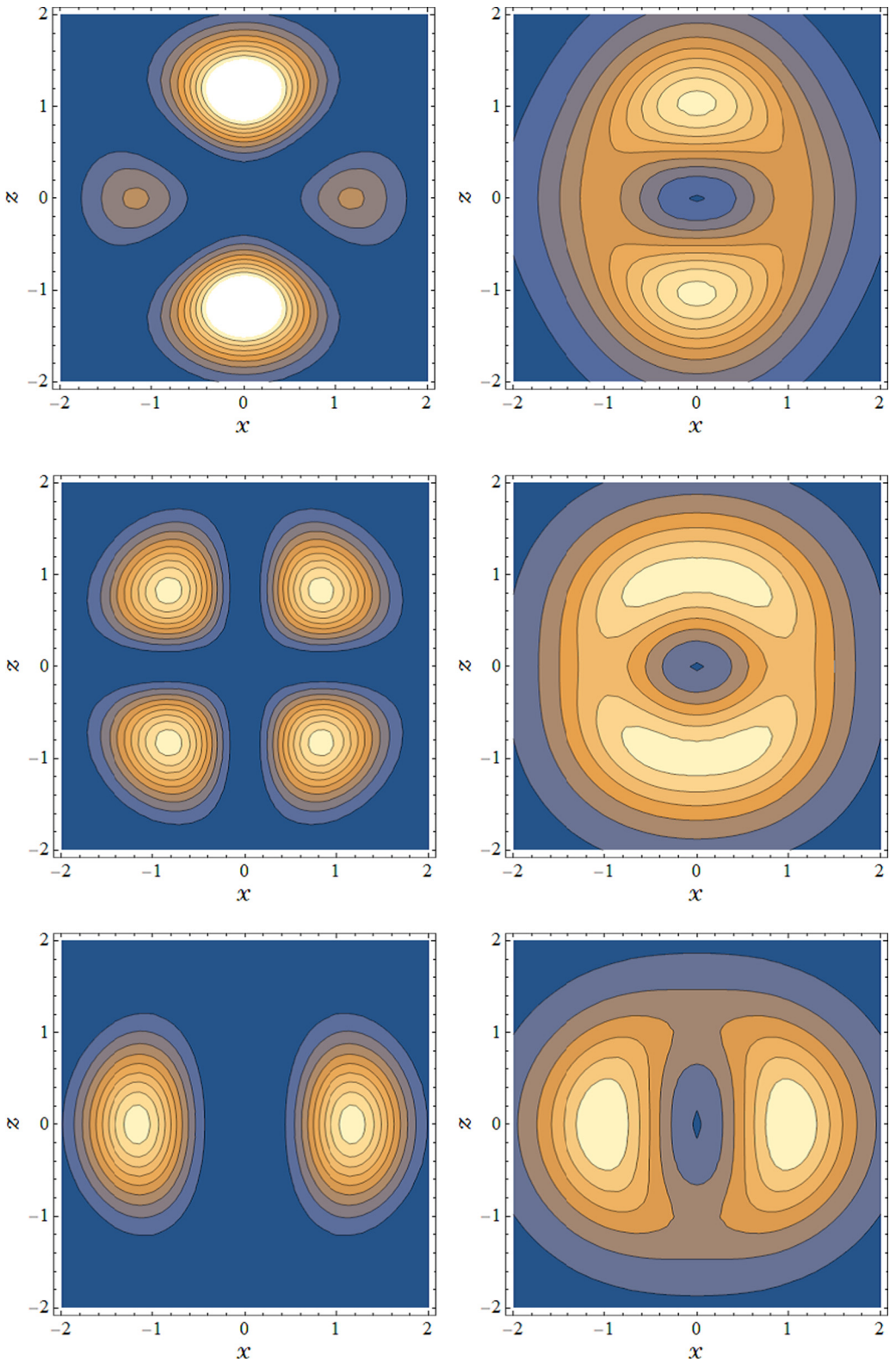

FIG. 6. The $J = 2$ contour plots of the impurity's probability density (left panel) and the real-space excited-boson distributions (right panel): the top, middle, and bottom panels are for $|J_z| = 0, 1, 2$. For other explanations, see the caption in Fig. 4.

or the indirect observation of the phase of the impurity's wave function, which has been done for the vortex state of the BEC [90], is also an interesting possibility. At the moment we have no fixed idea how to give a definite amount of angular momentum, but we think that a significant change in boson's distribution can be observed with the methods as discussed here. Also, in the observation of the excited bosons, the photon absorption spectra mentioned above may work out for

bosons as well. In addition, we think that *in situ* experiments may also work to get images of excited bosons [65,92–96], although it would be a challenge since the total excited-boson number per impurity is quite small.

ACKNOWLEDGMENTS

We are grateful to Kei Iida, Junichi Takahashi, and Ryosuke Imai for useful discussions on excitation spectra of interacting bosons in inhomogeneous systems, and to Kota Yanase for comments on angular momentum structure of excited nuclei. E.N. and H.Y. are supported by Grants-in-Aid for Scientific Research through Grants No. 17K05445 and No. 18K03501, respectively, provided by JSPS.

APPENDIX A: EXPECTATION VALUES OF OPERATORS BY THE COHERENT STATES

In this Appendix we present the expectation values of the gauge-transformed operators $S^{-1}\hat{J}^2 S$ and $S^{-1}\mathcal{H}S$, which are defined in (19) and (21), with respect to the coherent state (22). Using the expectation values of $\hat{M}_i$ and $\hat{L}_i$:

$$\langle \hat{M}_i \rangle_b = 0, \tag{A1}$$

$$\langle \hat{M}_{\pm 1}\hat{M}_{\mp 1}\rangle_b = \langle l,0\,|\,\hat{\mathcal{L}}_{\pm 1}\hat{\mathcal{L}}_{\mp 1}\,|\,l,0\rangle |f_{nl}|^2 = -\frac{l(l+1)}{2}|f_{nl}|^2, \tag{A2}$$

and $\langle \hat{M}_i\hat{M}_j\rangle_b = 0$ for the other combinations of i and j, we obtain the expectation value of the shift operator:

$$\begin{aligned}
\langle \hat{O}_L\rangle_b &= \langle S^{-1}(\hat{L}^2 S)\rangle_b \\
&= \left\langle -\frac{\cot\theta}{\sqrt{2}}(\hat{M}_{-1}+\hat{M}_{+1}) - \frac{1}{2}(\hat{M}_{-1}+\hat{M}_{+1})^2 + \frac{1}{\sin^2\theta}\left[\cos\theta\hat{M}_0 - \sin\theta\frac{1}{\sqrt{2}}(\hat{M}_{-1}-\hat{M}_{+1})\right]^2\right\rangle_b \\
&= -\frac{1}{2}\langle(\hat{M}_{-1}+\hat{M}_{+1})^2\rangle_b + \frac{1}{2}\langle(\hat{M}_{-1}-\hat{M}_{+1})^2\rangle_b = l(l+1)|f_{nl}|^2.
\end{aligned} \tag{A3}$$

Then the expectation value of the transformed squared total angular momentum operators becomes

$$\begin{aligned}
\langle S^{-1}\hat{J}^2 S\rangle_b &= \langle \hat{L}^2\rangle_b + \langle \hat{M}^2\rangle_b + \langle \hat{O}_L\rangle_b + 2\sum_{i,j} D^1_{i,j}(\varphi,\theta,0)\langle \hat{M}_j^\dagger[S^{-1}(\hat{L}_i S) + \hat{L}_i]\rangle_b \\
&= \hat{L}^2 + l(l+1)|f_{nl}|^2 + l(l+1)|f_{nl}|^2 + 2\sum_{i,j} D^1_{i,j}(\varphi,\theta,0)\langle \hat{M}_j^\dagger S^{-1}(\hat{L}_i S)\rangle_b \\
&= \hat{L}^2 + 2l(l+1)|f_{nl}|^2 - 2\sum_{i=0,\pm1}\left\{D^1_{i,-1}(\varphi,\theta,0)\langle \hat{M}_{+1}S^{-1}(\hat{L}_i S)\rangle_b + D^1_{i,+1}(\varphi,\theta,0)\langle \hat{M}_{-1}S^{-1}(\hat{L}_i S)\rangle_b\right\} \\
&= \hat{L}^2.
\end{aligned} \tag{A4}$$

Finally, we obtain the expectation value of the transformed Hamiltonian:

$$\langle S^{-1}\mathcal{H}S\rangle_b = H_{\rm ho}(\mathbf{r}) + \frac{l(l+1)|f_{nl}|^2}{2m_f r^2} + E^b_{00}N_0 + {\sum_{n,l}}' E^b_{nl}|f_{nl}|^2 + gN_0|\phi^b_0(\mathbf{r})|^2 + g\frac{\sqrt{N_0}}{4\pi}{\sum_{n,l}}'\sqrt{2l+1}R^b_{00}(r)R^b_{nl}(r)[f_{nl}+f^*_{nl}]. \tag{A5}$$

APPENDIX B: THE VARIATIONAL ENERGY FUNCTIONAL IN TERMS OF DIMENSIONLESS VARIABLES

Here we present the coefficients appearing in the functionals (29) and (30). The functional $G[F_{0J};F_{1J}]$ is expanded as

$$G[F_{0J};F_{1J}] := \int_{\mathbf{r}}\frac{1}{r^2}\left|\sum_{n=0,1}F_{nJ}\phi^I_{nJJ_z}(\mathbf{r})\right|^2 = |F_{0J}|^2G^0_J + F^*_{0J}F_{1J}G^c_J + F^*_{1J}F_{0J}G^{c*}_J + |F_{1J}|^2G^1_J, \tag{B1}$$

where the factors G^0_J, G^1_J, G^c_J is given as $G^0_J = G^1_J = G^c_J\sqrt{J+\frac{3}{2}} = \frac{\omega_I m_I}{J+\frac{1}{2}}$.

The another functional $H[F_{0J};F_{1J}]_{nl}$ is represented as

$$H[F_{0J};F_{1J}]_{nl} := \int_{\mathbf{r}}R^b_{00}(r)R^b_{nl}(r)\left|\sum_{n=0,1}F_{nJ}\phi^I_{nJJ_z}(\mathbf{r})\right|^2 = |F_{0J}|^2H^0_{nlJ} + F^*_{0J}F_{1J}H^c_{nlJ} + F^*_{1J}F_{0J}H^{c\,*}_{nlJ} + |F_{1J}|^2H^1_{nlJ}, \tag{B2}$$

where

$$H^0_{nlJ} = \int_0^\infty dr r^2 R^b_{00}(r) R^b_{nl}(r) R^I_{0J}(r)^2 = (m_I\omega_I)^{3/2}\mathcal{N}_{00}\mathcal{N}_{nl}\mathcal{N}^2_{0J}Q^{2J}\int_0^\infty dx x^{2+l+2J}\, e^{-(1+Q^2)x^2} L_n^{(\frac{1+2l}{2})}(x^2)$$
$$= (m_I\omega_I)^{3/2}\mathcal{N}_{00}\mathcal{N}_{nl}\mathcal{N}^2_{0J}Q^{2J}(1+Q^2)^{-\frac{3}{2}-J-\frac{l}{2}}\frac{\Gamma\left[\frac{3+2J+l}{2}\right]\Gamma\left[\frac{3+2l+2n}{2}\right]}{2\Gamma\left[\frac{3+2l}{2}\right]n!}F\left(\frac{3+2J+l}{2}, -n, \frac{3+2l}{2}, \frac{1}{1+Q^2}\right), \tag{B3}$$

$$H^c_{nlJ} = \int_0^\infty dr r^2 R^b_{00}(r) R^b_{nl}(r) R^I_{0J}(r) R^I_{1J}(r)$$
$$= (m_I\omega_I)^{3/2}\mathcal{N}_{00}\mathcal{N}_{nl}\mathcal{N}_{0J}\mathcal{N}_{1J}Q^{2J}\int_0^\infty dx x^{2+l+2J}\, e^{-(1+Q^2)x^2} L_n^{(\frac{1+2l}{2})}(x^2) L_1^{(\frac{1+2J}{2})}(Q^2x^2), \tag{B4}$$

$$H^1_{nlJ} = \int_0^\infty dr r^2 R^b_{00}(r) R^b_{nl}(r) R^I_{1J}(r)^2$$
$$= (m_I\omega_I)^{3/2}\mathcal{N}_{00}\mathcal{N}_{nl}\mathcal{N}^2_{1J}Q^{2J}\int_0^\infty dx x^{2+l+2J}\, e^{-(1+Q^2)x^2} L_n^{(\frac{1+2l}{2})}(x^2)\,\{L_1^{(\frac{1+2J}{2})}(Q^2x^2)\}^2, \tag{B5}$$

where $Q = \sqrt{\frac{m_I\omega_I}{m_b\omega_b}}$. The $\Gamma(z)$ and $F(a, b, c, z)$ in the above formulas represent the gamma and Gauss's hypergeometric functions, respectively. We have shown the analytic expression only for H^0_{nlJ}, but the remaining factors H^c_{nlJ} and H^1_{nlJ} also have similar analytic expressions, which are not presented here because they are lengthy and cumbersome.

In terms of dimensionless variables, the polaron binding energy [the energy shift (35)], defined by the energy difference of the systems with and without the impurity-medium interaction, is given by

$$\frac{\Delta E[F_{1J}]}{\omega_b} = 2\beta F^2_{1J} + \frac{N_0}{2}(1+\alpha)\alpha^{1/2}\beta^{3/2}\gamma\left[\tilde{H}^0_{00J} + 2F_{1J}\sqrt{1-F^2_{1J}}\tilde{H}^c_{00J} + F^2_{1J}\left(\tilde{H}^1_{00J} - \tilde{H}^0_{00J}\right)\right]$$
$$- \frac{N_0}{4}(1+\alpha)^2\alpha\beta^3\gamma^2\sum_{n,l}{}'(2l+1)\frac{\left[\tilde{H}^0_{nlJ} + 2F_{1J}\sqrt{1-F^2_{1J}}\tilde{H}^c_{nlJ} + F^2_{1J}\left(\tilde{H}^1_{nlJ} - \tilde{H}^0_{nlJ}\right)\right]^2}{\frac{3+2l+4n}{2} + \frac{l(l+1)}{2(J+\frac{1}{2})}\beta\left[1 + 2F_{1J}\sqrt{1-F^2_{1J}}\left(J+\frac{3}{2}\right)^{-1/2}\right]},$$
$$= 2\beta F^2_{1J} - \frac{3\sqrt{N_0}}{2}\bar{f}_{00}[F_{1J}] - \sum_{n,l}{}'\bar{f}_{nl}[F_{1J}]^2\left[\frac{3+2l+4n}{2} + \frac{l(l+1)}{2J+1}\beta\left(1 + 2\frac{F_{1J}\sqrt{1-F^2_{1J}}}{\sqrt{J+\frac{3}{2}}}\right)\right], \tag{B6}$$

where we have used the formal solution (31):

$$\bar{f}_{nl}[F_{1J}] = -\frac{\sqrt{N_0}}{2}(1+\alpha)\alpha^{1/2}\beta^{3/2}\gamma\sqrt{2l+1}\frac{\tilde{H}^0_{nlJ} + 2F_{1J}\sqrt{1-F^2_{1J}}\tilde{H}^c_{nlJ} + F^2_{1J}\left(\tilde{H}^1_{nlJ} - \tilde{H}^0_{nlJ}\right)}{\frac{3+2l+4n}{2} + \frac{l(l+1)}{2(J+\frac{1}{2})}\beta\left[1 + 2F_{1J}\sqrt{1-F^2_{1J}}\left(J+\frac{3}{2}\right)^{-1/2}\right]}, \tag{B7}$$

with $\tilde{H}^0_{nlJ} \equiv H^0_{nlJ}/(m_I\omega_I)^{3/2}$ and so on, $\alpha \equiv m_I/m_b$, $\beta \equiv \omega_I/\omega_b$, and $\gamma \equiv a(m_b\omega_b)^{1/2}$ via

$$\frac{g}{\omega_b}(m_I\omega_I)^{3/2} = \frac{2\pi a(m_b+m_I)}{m_bm_I}\frac{(m_I\omega_I)^{3/2}}{\omega_b} = 2\pi\left(1+\frac{m_I}{m_b}\right)\frac{\omega_I}{\omega_b}a(m_I\omega_I)^{1/2}$$
$$= 2\pi\left(1+\frac{m_I}{m_b}\right)\left(\frac{m_I}{m_b}\right)^{1/2}\left(\frac{\omega_I}{\omega_b}\right)^{3/2}a(m_b\omega_b)^{1/2}$$
$$= 2\pi(1+\alpha)\alpha^{1/2}\beta^{3/2}\gamma. \tag{B8}$$

APPENDIX C: THE GROUND-STATE ENERGY IN THE SECOND-ORDER PERTURBATION THEORY

In this Appendix we briefly show the derivation of the ground-state energy (37) obtained in the second-order perturbation theory. The Fröhlich-type Hamiltonian (1) in the full second-quantized form is represented as $\mathcal{H} = \mathcal{H}_0 + \mathcal{V}$, where the nonperturbative and perturbative parts $\mathcal{H}_0$ and $\mathcal{V}$ are defined as

$$\mathcal{H}_0 = \sum_u E^I_u a^\dagger_u a_u + E^b_0 N_0 + \sum_{s\neq 0} E^b_s b^\dagger_s b_s, \tag{C1}$$

$$\mathcal{V} = gN_0\sum_{u,u'} C_{00;uu'}a^\dagger_u a_{u'} + g\sqrt{N_0}\sum_{s\neq 0,u,u'}(C_{0s;uu'}b_s + C_{s0;uu'}b^\dagger_s)a^\dagger_u a_{u'}, \tag{C2}$$

where a_u ($a_u^\dagger$) is the annihilation (creation) operator of impurity with the labels of the abbreviated form $u = (n, l, m)$, and, also, the ground state is represented by $u = 0$. The overlap integrals $C_{ss';uu'}$ of the wave functions are defined by

$$C_{ss';uu'} = \int_{\mathbf{r}} \phi_s^{b*}(\mathbf{r})\phi_{s'}^{b}(\mathbf{r})\phi_u^{I*}(\mathbf{r})\phi_{u'}^{I}(\mathbf{r}). \tag{C3}$$

In the diagrammatic method of the perturbation theory, the ground state energy is obtained from the summation of the connected diagrams (Goldstone's theorem). Up to the second order of g for $J = J_z = 0$, it becomes

$$\begin{aligned}
\langle \mathcal{H} \rangle &= \langle \Phi_0|\mathcal{H}_0|\Phi_0\rangle + \langle \Phi_0|\mathcal{V}|\Phi_0\rangle + \sum_i \frac{\langle \Phi_0|\mathcal{V}|i\rangle \langle i|\mathcal{V}|\Phi_0\rangle}{\langle \Phi_0|\mathcal{H}_0|\Phi_0\rangle - \langle i|\mathcal{H}_0|i\rangle} \\
&= E_0^f + E_0^b N_0 + gN_0 C_{00;00} + \sum_{s\neq 0,u} \frac{|\langle 0|b_s a_u \mathcal{V} a_0^\dagger|0\rangle|^2}{E_0^I + E_0^b N_0 - \langle 0|b_s a_u \left(\sum_{u'} E_{u'}^I a_{u'}^\dagger a_{u'} + E_0^b N_0 + \sum_{s'}' E_{s'}^b b_{s'}^\dagger b_{s'}\right) a_u^\dagger b_s^\dagger|0\rangle} \\
&\quad + \sum_{u\neq 0} \frac{|\langle 0|a_u \mathcal{V} a_0^\dagger|0\rangle|^2}{E_0^I + E_0^b N_0 - \langle 0|a_u \left(\sum_{u'} E_{u'}^I a_{u'}^\dagger a_{u'} + E_0^b N_0 + \sum_{s'}' E_{s'}^b b_{s'}^\dagger b_{s'}\right) a_u^\dagger|0\rangle} \\
&= E_0^I + E_0^b N_0 + gN_0 C_{00;00} - g^2 N_0 \sum_{s\neq 0,u} \frac{C_{0s;0u}C_{s0;u0}}{E_u^I - E_0^I + E_s^b} - g^2 N_0^2 \sum_{u\neq 0} \frac{C_{00;0u}C_{00;u0}}{E_u^I - E_0^I},
\end{aligned} \tag{C4}$$

where the nonperturbative ground state are defined by

$$|\Phi_0\rangle = a_0^\dagger |0\rangle, \tag{C5}$$

with the Fock vacuum of excited bosons $|0\rangle$ (the condensed state of the lowest-energy boson), and the intermediate states $|i\rangle$ are

$$|i\rangle = \{a_u^\dagger b_{s\neq 0}^\dagger |0\rangle,\ a_{u\neq 0}^\dagger |0\rangle\}. \tag{C6}$$

In order to make a fair comparison with the variational method, in the ground-state energy formula ($J = 0$) we take the impurity intermediate states up to $u = (1, 0, 0)$, and those of bosons only for $l = m = 0$ (consistent with the $J = 0$ state). Then we obtain the ground-state energy in the second-order perturbation theory:

$$\langle \mathcal{H} \rangle \simeq E_{00}^I + E_{00}^b N_0 + g\frac{N_0}{4\pi} H_{000}^0 - g^2 \frac{N_0}{(4\pi)^2} \sum_{n\neq 0} \left(\frac{|H_{n00}^c|^2}{E_{10}^I - E_{00}^I + E_{n0}^b} + \frac{|H_{n00}^0|^2}{E_{n0}^b} \right) - g^2 \left(\frac{N_0}{4\pi}\right)^2 \frac{|H_{000}^c|^2}{E_{10}^I - E_{00}^I}, \tag{C7}$$

which is just Eq. (37).

[1] J. Catani, G. Lamporesi, D. Naik, M. Gring, M. Inguscio, F. Minardi, A. Kantian, and T. Giamarchi, Phys. Rev. A **85**, 023623 (2012).

[2] R. Scelle, T. Rentrop, A. Trautmann, T. Schuster, and M. K. Oberthaler, Phys. Rev. Lett. **111**, 070401 (2013).

[3] M. Hohmann, F. Kindermann, B. Gänger, T. Lausch, D. Mayer, F. Schmidt, and A. Widera, EPJ Quantum Technol. **2**, 23 (2015)

[4] E. Compagno, G. De Chiara, D. G. Angelakis, and G. M. Palma, Sci. Rep. **7**, 2355 (2017).

[5] N. B. Jørgensen, L. Wacker, K. T. Skalmstang, M. M. Parish, J. Levinsen, R. S. Christensen, G. M. Bruun, and J. J. Arlt, Phys. Rev. Lett. **117**, 055302 (2016).

[6] M.-G. Hu, M. J. Van de Graaff, D. Kedar, J. P. Corson, E. A. Cornell, and D. S. Jin, Phys. Rev. Lett. **117**, 055301 (2016).

[7] T. Rentrop, A. Trautmann, F. A. Olivares, F. Jendrzejewski, A. Komnik, and M. K. Oberthaler, Phys. Rev. X **6**, 041041 (2016).

[8] B. Fröhlich, M. Feld, E. Vogt, M. Koschorreck, W. Zwerger, and M. Köhl, Phys. Rev. Lett. **106**, 105301 (2011).

[9] F. Scazza, G. Valtolina, P. Massignan, A. Recati, A. Amico, A. Burchianti, C. Fort, M. Inguscio, M. Zaccanti, and G. Roati, Phys. Rev. Lett. **118**, 083602 (2017).

[10] M. Cetina, M. Jag, R. S. Lous, I. Fritsche, J. T. M. Walraven, R. Grimm, J. Levinsen, M. M. Parish, R. Schmidt, M. Knap, and E. Demler, Science **354**, 96 (2016).

[11] C. J. Pethick and H. Smith, *Bose-Einstein Condensation in Dilute Gases* (Cambridge University Press, Cambridge, 2008).

[12] L. Pitaevskii and S. Stringari, *Bose-Einstein Condensation* (Oxford, New York, 2003).

[13] F. M. Cucchietti and E. Timmermans, Phys. Rev. Lett. **96**, 210401 (2006).

[14] K. Sacha and E. Timmermans, Phys. Rev. A **73**, 063604 (2006).

[15] J. Tempere, W. Casteels, M. K. Oberthaler, S. Knoop, E. Timmermans, and J. T. Devreese, Phys. Rev. B **80**, 184504 (2009).

[16] W. Casteels, T. Van Cauteren, J. Tempere, and J. T. Devreese, Laser Phys. **21**, 1480 (2011).

[17] S. P. Rath and R. Schmidt, Phys. Rev. A **88**, 053632 (2013)

[18] A. Shashi, F. Grusdt, D. A. Abanin, and E. Demler, Phys. Rev. A **89**, 053617 (2014).

[19] W. Li and S. Das Sarma, Phys. Rev. A **90**, 013618 (2014).

[20] J. Levinsen, M. M. Parish, and G. M. Bruun, Phys. Rev. Lett. **115**, 125302 (2015).

[21] A. S. Dehkharghani, A. G. Volosniev, and N. T. Zinner, Phys. Rev. A **92**, 031601(R) (2015).
[22] L. A. Peña Ardila and S. Giorgini, Phys. Rev. A **92**, 033612 (2015).
[23] R. S. Christensen, J. Levinsen, and G. M. Bruun, Phys. Rev. Lett. **115**, 160401 (2015)
[24] J. Vlietinck, W. Casteels, K. Van Houcke, J. Tempere, J. Ryckebusch, and J. T. Devreese, New J. Phys. **17**, 033023 (2015).
[25] F. Grusdt, Y. E. Shchadilova, A. N. Rubtsov, and E. Demler, Sci. Rep. **5**, 12124 (2015).
[26] F. Grusdt and M. Fleischhauer, Phys. Rev. Lett. **116**, 053602 (2016).
[27] Y. E. Shchadilova, F. Grusdt, A. N. Rubtsov, and E. Demler, Phys. Rev. A **93**, 043606 (2016).
[28] Y. E. Shchadilova, R. Schmidt, F. Grusdt, and E. Demler, Phys. Rev. Lett. **117**, 113002 (2016).
[29] F. Grusdt, K. Seetharam, Y. Shchadilova, and E. Demler, Phys. Rev. A **97**, 033612 (2018).
[30] Y. Ashida, R. Schmidt, L. Tarruell, and E. Demler, Phys. Rev. B **97**, 060302(R) (2018).
[31] L. A. Peña Ardila, N. B. Jörgensen, T. Pohl, S. Giorgini, G. M. Bruun, and J. J. Arlt, arXiv:1812.04609.
[32] K. K. Nielsen, L. A. Pena Ardila, G. M. Bruun, and T. Pohl, New J. Phys. (to be published).
[33] S. I. Mistakidis, A. G. Volosniev, N. T. Zinner, and P. Schmelcher, arXiv:1809.01889.
[34] S. I. Mistakidis, G. C. Katsimiga, G. M. Koutentakis, T. Busch, and P. Schmelcher, arXiv:1811.10702.
[35] See, for instance, A. S. Alexandrov, and J. T. Devreese, in *Advances in Polaron Physics*, Springer Series in Solid-State Sciences Vol. 159 (Springer, New York, 2009).
[36] L. Landau and S. Pekar, J. Exptl. Theor. Phys. **18**, 419 (1948); S. Pekar, *ibid.* **19**, 796 (1949).
[37] H. Fröhlich, *Theory of Dielectrics* (Clarendon, Oxford, 1949); H. Fröhlich, H. Pelzer, and S. Zienau, Philos. Mag. **41**, 221 (1950); H. Fröhlich, Adv. Phys. **3**, 325 (1954).
[38] F. Chevy, Phys. Rev. A **74**, 063628 (2006); M. Inguscio, W. Ketterle, and C. Salomon (Eds.), *Ultra-Cold Fermi Gases* (IOS, Amsterdam, 2007), p. 607.
[39] P. Massignan, G. M. Bruun, and H. T. C. Stoof, Phys. Rev. A **78**, 031602(R) (2008).
[40] A. Schirotzek, C.-H. Wu, A. Sommer, and M. W. Zwierlein, Phys. Rev. Lett. **102**, 230402 (2009).
[41] M. Ku, J. Braun, and A. Schwenk, Phys. Rev. Lett. **102**, 255301 (2009).
[42] R. Schmidt and T. Enss, Phys. Rev. A **83**, 063620 (2011).
[43] C. Kohstall, M. Zaccanti, M. Jag, A. Trenkwalder, P. Massignan, G. M. Bruun, F. Schreck, and R. Grimm, Nature (London) **485**, 615 (2012).
[44] M. Koschorreck, D. Pertot, E. Vogt, B. Fröhlich, M. Feld, and M. Köhl, Nature (London) **485**, 619 (2012).
[45] R. Schmidt, T. Enss, V. Pietilä, and E. Demler, Phys. Rev. A **85**, 021602(R) (2012).
[46] J. Vlietinck, J. Ryckebusch, and K. Van Houcke, Phys. Rev. B **87**, 115133 (2013).
[47] C. Trefzger and Y. Castin, Europhys. Lett. **104**, 50005 (2013).
[48] C. Trefzger and Y. Castin, Phys. Rev. A **90**, 033619 (2014).
[49] P. Massignan, M. Zaccanti, and G. M. Bruun, Rep. Prog. Phys. **77**, 034401 (2014).
[50] Z. Lan and C. Lobo, J. Indian Inst. Sci. **94**, 179 (2014).
[51] Z. Lan and C. Lobo, Phys. Rev. A **92**, 053605 (2015).
[52] F. N. Ünal, B. Hetényi, and M. Ö. Oktel, Phys. Rev. A **91**, 053625 (2015).
[53] W. Yi and X. Cui, Phys. Rev. A **92**, 013620 (2015).
[54] M. M. Parish and J. Levinsen, Phys. Rev. B **94**, 184303 (2016).
[55] J. Levinsen, P. Massignan, S. Endo, and M. M. Parish, J. Phys. B: At. Mol. Opt. Phys. **50**, 072001 (2017).
[56] K. Kamikado, T. Kanazawa, and S. Uchino, Phys. Rev. A **95**, 013612 (2017).
[57] B. Kain and H. Y. Ling, Phys. Rev. A **96**, 033627 (2017)
[58] R. Schmidt, M. Knap, D. A. Ivanov, J.-S. You, M. Cetina, and E. Demler, Rep. Prog. Phys. **81**, 024401 (2018).
[59] S. I. Mistakidis, G. C. Katsimiga, G. M. Koutentakis, and P. Schmelcher, arXiv:1808.00040.
[60] J. Levinsen, P. Massignan, F. Chevy, and C. Lobo, Phys. Rev. Lett. **109**, 075302 (2012).
[61] T.-S. Deng, Z.-C. Lu, Y.-R. Shi, J.-G. Chen, W. Zhang, and W. Yi, Phys. Rev. A **97**, 013635 (2018).
[62] B. Kain and H. Y. Ling, Phys. Rev. A **89**, 023612 (2014).
[63] L. A. Peña Ardila and T. Pohl, J. Phys. B: At. Mol. Opt. Phys. **52**, 015004 (2018).
[64] H. Tajima and S. Uchino, New J. Phys. **20**, 073048 (2018).
[65] Z. Yan, P. B. Patel, B. Mukherjee, R. J. Fletcher, J. Struck, and M. W. Zwierlein, Phys. Rev. Lett. **122**, 093401 (2018).
[66] H. Tajima and S. Uchino, arXiv:1812.05889.
[67] J. Levinsen, M. M. Parish, R. S. Christensen, J. J. Arlt, and G. M. Bruun, Phys. Rev. A **96**, 063622 (2017).
[68] N.-E. Guenther, P. Massignan, M. Lewenstein, and G. M. Bruun, Phys. Rev. Lett. **120**, 050405 (2018).
[69] M. Bruderer, A. Klein, S. R. Clark, and D. Jaksch, Phys. Rev. A **76**, 011605(R) (2007); New J. Phys. **10**, 033015 (2008).
[70] E. Nakano and H. Yabu, Phys. Rev. B **93**, 205144 (2016).
[71] For instance, see, D. J. Rowe, *Nuclear Collective Motion: Models and Theory* (World Scientific, New Jersey, 2010).
[72] D. R. Inglis, Phys. Rev. **96**, 1059 (1954); **97**, 701 (1955).
[73] D. J. Thouless and J. G. Valatin, Nucl. Phys. **31**, 211 (1962).
[74] R. Schmidt and M. Lemeshko, Phys. Rev. Lett. **114**, 203001 (2015).
[75] R. Schmidt and M. Lemeshko, Phys. Rev. X **6**, 011012 (2016).
[76] E. Yakaboylu, B. Midya, A. Deuchert, N. Leopold, and M. Lemeshko, Phys. Rev. B **98**, 224506 (2018).
[77] E. Nakano, H. Yabu, and K. Iida, Phys. Rev. A **95**, 023626 (2017)
[78] M. E. Rose, *Elementary Theory of Angular Momentum* (Dover, New York, 2011).
[79] T. D. Lee, F. E. Low, and D. Pines, Phys. Rev. **90**, 297 (1953).
[80] S. S. Schweber, *An Introduction to Relativistic Quantum Field Theory* (Dover, New York, 2005).
[81] A. R. Edmonds, *Angular Momentum in Quantum Mechanics* (Princeton University Press, Princeton, NJ, 1957).
[82] F. Dalfovo, S. Giorgini, L. P. Pitaevskii, and S. Stringari, Rev. Mod. Phys. **71**, 463 (1999).
[83] Y. Japha and Y. B. Band, Phys. Rev. A **84**, 033630 (2011).
[84] N. N. Bogoliubov, J. Phys. (USSR) **11**, 23 (1947).
[85] P. G. de Gennes, *Superconductivity of Metals and Alloys* (Benjamin, New York, 1966).
[86] M. Lewenstein and L. You, Phys. Rev. Lett. **77**, 3489 (1996).
[87] Y. Nakamura, J. Takahashi, and Y. Yamanaka, Phys. Rev. A **89**, 013613 (2014).

[88] Y. Nakamura, T. Kawaguchi, Y. Torii, and Y. Yamanaka, Ann. Phys. **376**, 484 (2017).
[89] A. Lampo, C. Charalambous, M. Á. García-March, and M. Lewenstein, Phys. Rev. A **98**, 063630 (2018).
[90] M. R. Matthews, B. P. Anderson, P. C. Haljan, D. S. Hall, C. E. Wieman, and E. A. Cornell, Phys. Rev. Lett. **83**, 2498 (1999).
[91] K. W. Madison, F. Chevy, W. Wohlleben, and J. Dalibard, Phys. Rev. Lett. **84**, 806 (2000); J. R. Abo-Shaeer, C. Raman, J. M. Vogels, and W. Ketterle, Science **292**, 476 (2001).
[92] Y.-I. Shin, C. H. Schunck, A. Schirotzek, and W. Ketterle, Nature (London) **451**, 689 (2008).
[93] W. S. Bakr, J. I. Gillen, A. Peng, S. Fölling, and M. Greiner, Nature (London) **462**, 74 (2009).
[94] J. F. Sherson, C. Weitenberg, M. Endres, M. Cheneau, I. Bloch, and S. Kuhr, Nature (London) **467**, 68 (2010).
[95] M. Horikoshi, S. Nakajima, M. Ueda, and T. Mukaiyama, Science **327**, 442 (2010).
[96] M. J. H. Ku, A. T. Sommer, L. W. Cheuk, and M. W. Zwierlein, Science **335**, 563 (2012).